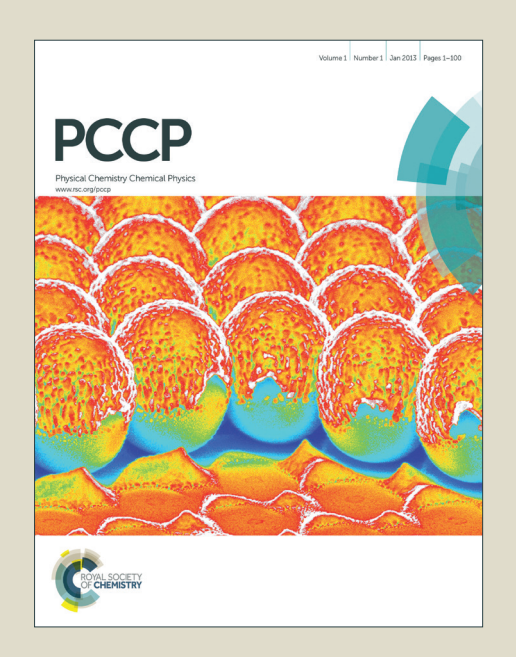


# Accepted Manuscript



This is an *Accepted Manuscript*, which has been through the Royal Society of Chemistry peer review process and has been accepted for publication.

Accepted Manuscripts are published online shortly after acceptance, before technical editing, formatting and proof reading. Using this free service, authors can make their results available to the community, in citable form, before we publish the edited article. We will replace this Accepted Manuscript with the edited and formatted Advance Article as soon as it is available.

You can find more information about *Accepted Manuscripts* in the **Information for Authors**.

Please note that technical editing may introduce minor changes to the text and/or graphics, which may alter content. The journal's standard <u>Terms & Conditions</u> and the <u>Ethical guidelines</u> still apply. In no event shall the Royal Society of Chemistry be held responsible for any errors or omissions in this *Accepted Manuscript* or any consequences arising from the use of any information it contains.



PCCP RSCPublishing

**ARTICLE** 

# Infrared Multiple Photon Dissociation Spectrum of Protonated Bis(2-methoxyethyl) Ether Obtained with a Tunable CO<sub>2</sub> Laser

M. U. Ehsan, Y. Bozai, W. L. Pearson,  $\mathrm{III}$ , N. A. Horenstein and J. R. Eyler\*

A moderate-resolution infrared multiple photon dissociation (IRMPD) spectrum of protonated bis(2-methoxyethyl) ether (diglyme) was obtained using a grating-tuned  $CO_2$  laser. The experimental spectrum compares well with one calculated theoretically at the MP2 level and exhibits defined peaks over the span of the  $CO_2$  laser output lines as opposed to a relatively featureless spectrum over this wavelength range obtained using free electron laser infrared radiation. The lowest energy structure corresponding to the calculated vibrational spectrum is consistent with structures previously calculated at the same level of theory. Alternative structures were calculated at lower levels of theory for comparison and investigation of the energetics of proton-heteroatom interactions. Broadening of the IRMPD action spectrum due to energetic phenomena characteristic of proton bridges was not observed and thus did not obscure the correlation between theoretical calculations and experimentally determined spectra as it may have in previous studies.

#### Introduction

The technique of infrared multiple photon dissociation (IRMPD) has been used increasingly in recent years (often in conjunction with theoretical calculations) to determine unambiguously the structure of a wide range of gaseous ions.1 In this approach an action spectrum is obtained by monitoring dissociation of an ion of interest as a function of the wavelength of the (tunable) infrared laser used to induce IRMPD. technique involves the slow, sequential absorption of photons by trapped ions, which causes a gradual increase in the internal energy of the ions until (in most cases) the lowest energy dissociation threshold is reached. The nature of the process has led to the widespread use of the term "multiple" photon dissociation, in contrast to the infrared "multi-photon" experiments that have applied powerful pulsed lasers to dissociate neutral species, often as a part of isotope separation schemes.2

Tunable infrared laser sources used for IRMPD spectroscopy experiments have included free electron lasers (FELs), 3,4 optical parametric oscillators/amplifiers (OPO/As), 4-8 and carbon dioxide (CO<sub>2</sub>) lasers, most often grating-tuned. 9-12 Ions under study and their IRMPD products are most often trapped and detected in Fourier transform ion cyclotron resonance (FTICR) mass spectrometers 3-7, 9, 10 or linear/quadrupole ion traps. 4,8,11,12

Bis(2-methoxyethyl) ether (diglyme) is a commonly used organic solvent. It was a convenient molecule for study in early IRMPD experiments since it is readily protonated via ion-molecule reactions with its electron ionization-produced fragments<sup>9-11</sup> and has a rich absorption spectrum in the mid-infrared due to its numerous C-O-C stretching and bending vibrations. Following very limited spectroscopic studies of protonated diglyme involving a few output wavelengths from a grating-tuned CO<sub>2</sub> laser, <sup>10,11</sup> more extensive mid-infrared spectra of that ion and related proton-bound dimers of small ethers and water were obtained using the Free Electron Laser for Infrared

# **RSCPublishing**

## **ARTICLE**

eXperiments (FELIX).<sup>13</sup> Theoretical calculations of low energy structures and infrared spectra of protonated diglyme were also reported in Ref. 13.

The experimental spectrum for protonated diglyme shown in Ref. 13 has quite broad peaks, with only a shoulder and two poorly resolved peaks spanning the entire output wavelength range of a tunable CO<sub>2</sub> laser  $(9.20 - 10.70 \, \mu \text{m} / 930 - 1090 \, \text{cm}^{-1})$ . Our earlier work<sup>10,11</sup> had reported a relatively well-defined peak in the 940 cm<sup>-1</sup> region for this ion. Broadening of the spectral peaks in FEL experiments is seen due to the wide bandwidth (~10 cm<sup>-1</sup> full-width at half maximum (FWHM) in this wavenumber range) of the FEL irradiation. By contrast the output lines of a gratingtuned CO<sub>2</sub> laser, separated from each other by ~2 cm<sup>-1</sup>, have a bandwidth of < 0.01 cm<sup>-1</sup>. Peak broadening seen in the earlier FEL work could also have been due in part to internal excitation of the protonated diglyme ions imparted during their formation by exoergic ionmolecule reactions with electron ionization-produced fragments. Electrospray ionization<sup>14</sup> (ESI) is a potentially "gentler" means of forming the protonated parent ions.

This paper reports a moderate resolution  $\mathrm{CO}_2$  laser-generated IRMPD spectrum of protonated diglyme, produced by electrospray ionization and trapped in an FTICR mass spectrometer, over the wavenumber range  $930-1090~\mathrm{cm}^{-1}$ . Reasonable agreement is seen between the experimental spectrum and one corresponding to the calculated lowest energy structure of the ion for which the proton asymmetrically bridges between the two methoxy oxygens of the diglyme molecule.

#### **Experimental and computational details**

#### Reagents and materials

Diglyme was obtained from Sigma-Aldrich Co. and Optima® LC/MS grade methanol, HPLC grade water, and aldehyde-free sequencing grade formic acid were obtained from Fisher Scientific. Diglyme samples were prepared at a concentration of 0.002M in a solution of 46.5:52.5:1% CH<sub>3</sub>OH:H<sub>2</sub>O:HCOOH. Due to instability in electrospray current during initial experiments with solutions of this concentration, the 0.002 M solutions were further diluted with 50:50% CH<sub>3</sub>OH:H<sub>2</sub>O to a concentration of 0.0004 M.

#### **Experimental set-up**

Protonated diglyme solutions were ionized using a commercial ESI source (Analytica of Branford; Branford, CT). The apparatus was modified with a

conical capillary inlet maintained at a temperature of 150 °C. <sup>15</sup> Typical ESI conditions included an infusion rate between 25 – 50  $\mu L$  h $^{-1}$  and a spray voltage of 2750 V. A Bruker 47e FTICR mass spectrometer (Bruker Daltonics; Billerica, MA) with a 4.7 T superconducting magnet (Magnex Scientific Ltd.; Abington, U.K.) and an Infinity Cell<sup>TM</sup> was used for experimentation. <sup>16</sup> Protonated diglyme (m/z 135.1) was mass isolated after formation by ESI, trapped in the FTICR analyzer cell, and irradiated with a Lasy-20G tunable continuous wave (cw) CO<sub>2</sub> laser (Access Laser Co.; Marysville, WA) with a wavelength range of 9.20 – 10.70  $\mu m$  and a power range of 0 – 8 W.

#### **Procedure**

The CO<sub>2</sub> laser irradiation wavelength and power were controlled with a LabVIEW-based (National Instruments; Austin, TX) laboratory-written software program<sup>17</sup> that was interfaced to the relevant control lines of the laser. This allowed convenient power selection and switching of wavelengths between experimental runs. Irradiation time was controlled by a Uniblitz electronic shutter (Vincent Associates; Rochester, NY). When the shutter was open, infrared light was allowed to pass through a coated ZnSe window on the opposite side of the vacuum chamber from the ion transfer optics and into the Infinity Cell<sup>TM</sup>. Because no internal mirrors were used, the ions were exposed to a single pass of infrared radiation. When the shutter was closed the laser beam was reflected from the polished shutter leaves onto a power meter to monitor the CW laser power.

At each wavelength, 5 sets of scans, which individually consisted of averaging 10 runs of 512 K ion transient response signals, were collected and averaged. As reported earlier,  $^{9-11,13}$  the major IRMPD fragment ion seen was at m/z 103.1 (nominal loss of CH<sub>3</sub>OH from the protonated parent), with an ion at m/z 59.1 occasionally seen for longer irradiation times and/or higher laser powers. For each CO<sub>2</sub> laser wavelength, a relative cross-section for dissociation was calculated from the power-corrected natural logarithm of the (P+F)/P ratio, where F corresponds to the combined relative abundance of m/z 103.1 and 59.1 ions and P is the relative abundance of the depleted protonated parent ion (m/z 135.1). The IRMPD action spectrum was obtained by plotting relative cross-section vs. laser wavenumber.

#### Reproducibility

Various portions of the spectrum shown in Fig. 1a were obtained repeatedly over the course of four

## **RSCPublishing**

## **ARTICLE**

months. Although keeping the average total abundance of ions within the cell and the measured laser power constant have been reported as effective means of ensuring reproducibility of the IRMPD process, <sup>18</sup> additional steps were taken in this work.

Irradiation power and irradiation time were adjusted so that the abundance ratio of the primary fragment ion (m/z 103.1) to the precursor ion (m/z 135.1) was 7:10 at an irradiation wavelength of 9.588 µm. This was done both at the beginning of experimentation for the day, and after the collection of 5 experimental scans (*vide supra*) for each wavelength used on that particular day. Irradiation time was modified slightly to maintain the 7:10 fragment:parent ratio, compensating for slight shifts during the course of the day in the ion cloud position, heating of cell plates by stray IR radiation, and other phenomena that affect the internal energy of the ions due to the ESI formation and mass spectrometric trapping processes.

In addition, the 9.588 µm wavelength was used for further normalization of the data due to its consistent and reliable intensity. Relative IRMPD cross-section values using this wavelength were collected each day throughout this study, making it an even more appropriate reference point for proper instrumental functioning. A consistent relative IRMPD crosssection value was observed, and any instrumental fluctuations were corrected by normalizing the crosssection values of 9.588 µm to this preset quantity. Thus, the 9.588 µm cross-section value from any given day was compared to this "standard" value, and a correction factor was generated to compensate for deviations in IRMPD fragmentation at this wavelength resulting from factors mentioned above. Since the instrumental and experimental fluctuations affected data collected for all wavelengths that day, the correction factor was applied to the cross-section value generated for each wavelength used that day for IRMPD experiments. A three-point running average was then applied to the averaged, scaled cross-section points for smoothing before the experimental IRMPD action spectrum was plotted.

#### Theoretical calculations

Calculations of the lowest energy ion structures and their corresponding harmonic vibrational frequencies utilized the Gaussian 09 suite of programs. <sup>19</sup> Initial work used density functional theory (DFT) employing Becke's three-parameter exchange potential and the Lee-Yang-Parr correlation functional (B3LYP) with a 6-311++G\*\* basis set. The lowest energy structure found with that approach was then further optimized using second order Møller-Plesset perturbation (MP2)

theory with a cc-pVDZ basis set, and a harmonic approximation infrared spectrum was generated from the calculated vibrational frequencies, applying the recommended<sup>20</sup> frequency scaling factor of 0.953.

#### **Results and discussion**

The experimental IRMPD action spectrum is shown in Fig. 1a, with the theoretically determined vibrational spectrum given in Fig. 1b for comparison. Wavenumber gaps in the IRMPD spectrum are seen for two reasons. First, even though the tunable  $CO_2$  laser output wavelengths range from ~9.20 to  $10.8~\mu m$ , output lines are actually produced in four distinct regions (9.192 – 9.354  $\mu m$ , 9.458 – 9.773  $\mu m$ , 10.115 – 10.365  $\mu m$ , and 10.458 – 10.835  $\mu m$ ), due to the rotational/vibrational transitions giving rise to the lasing action. Second, some of the output lines at the extremes of these regions did not have sufficient power to dissociate the protonated diglyme in a reproducible manner, so no data were collected for those lines.

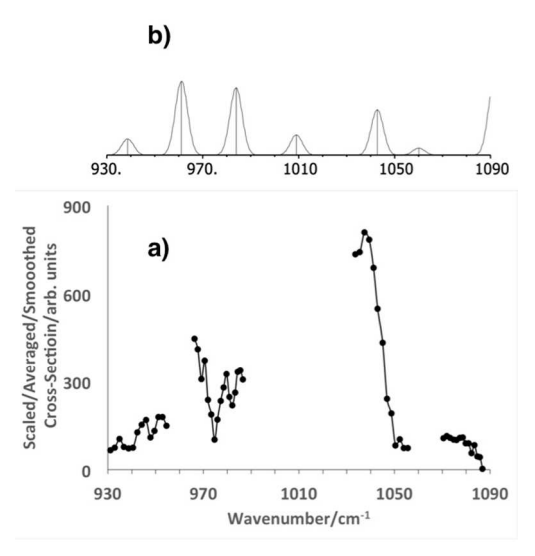


Fig. 1 a) Experimental IRMPD spectrum of protonated diglyme over the output range of a line-tunable  $CO_2$  laser, and b) theoretically calculated (MP2 cc-pVDZ) harmonic vibrational spectrum for the same wavenumber range. Calculated vibrational frequencies were scaled by 0.953 and peaks were convoluted with a 3 cm $^{-1}$  half-width Gaussian line shape.

The experimental spectrum contains one strong peak at ~1040 cm<sup>-1</sup>, what appear to be the shoulders of

# **RSCPublishing**

## **ARTICLE**

two other peaks in the 965 - 990 cm<sup>-1</sup> region, and evidence for one or more peaks of low intensity in the 930 – 960 cm<sup>-1</sup> region. There is considerably more detail seen in this (partial) spectrum than was reported in the earlier<sup>13</sup> IRMPD spectrum produced by FELIX, which had very broad features in the 930 – 1100 cm<sup>-1</sup> range, presumably for reasons discussed in the The small peaks in the lowest Introduction. wavenumber region in Fig. 1a are at approximately the same wavenumber but not identical in shape when compared to those reported in Refs. 10 and 11. However, different CO<sub>2</sub> lasers and mass spectrometers, as well as electron ionization rather than ESI, were used in the earlier work, which could result in small shifts in the position and bandwidth of the IRMPD spectral peaks.

There is reasonable agreement between the experimental and theoretical spectra for the four peaks at ~940, 960, 985, and 1040 cm<sup>-1</sup>. The predicted peaks at 1010 and 1060 cm<sup>-1</sup>, as well as one at ~1095 cm<sup>-1</sup> are unfortunately at positions for which there are no CO<sub>2</sub> laser output lines. The lack of agreement in intensities of the experimental vs. theoretical peaks is commonly seen for IRMPD spectra, since single-photon absorption spectra are calculated while multiple photons are absorbed in the IRMPD process.

The calculated lowest energy structure corresponding to the theoretical vibrational spectrum in Fig. 1b is shown in Fig. 2. The proton is predicted

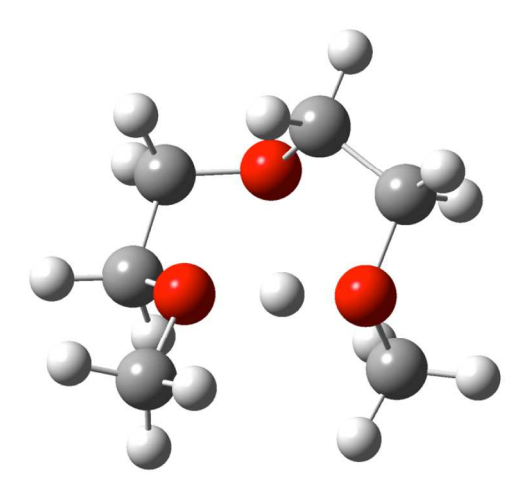


Fig. 2 Calculated (MP2 cc-pVDZ) lowest energy structure of protonated diglyme corresponding to the vibrational spectrum in Fig. 1b).

to be located asymmetrically between the two methoxy oxygen atoms (1.12  $\rm \mathring{A}$  from one and 1.31  $\rm \mathring{A}$  from the other), with an O-H-O bond angle of 177°.

The distance between the proton and the central oxygen atom of the diglyme molecule is calculated to be 2.44 Å. As would be expected, this structure is virtually identical to the lowest energy structure shown in Ref. 13, also calculated via MP2 (cc-pVDZ).

Alternative theoretical structures and their energetics have been investigated both previously and in this study. Ref. 13 described calculation of the energy of a structure in which the proton was symmetrically located between the two methoxy oxygen atoms and found it to be ~6 kcal mol<sup>-1</sup> higher than that of the asymmetric structure. In the initial stages of this study, we used DFT calculations to compare the relative energies of the "bidentate" structure shown in Fig. 2 with two "tridentate" structures, one with  $C_{2v}$  symmetry and one asymmetric, in which the proton was more closely equidistant from all three diglyme oxygen atoms. We thought it possible that interaction of the proton with the lone pairs on three oxygen atoms might be more energetically favorable than interaction with lone pairs on only the two methoxy oxygens. However, these two structures were found to be respectively 6.3 and 7.7 kcal mol<sup>-1</sup> higher in energy (zero-point corrected) than the "bidentate" structure shown in Fig. 2.

In Ref. 13, IRMPD spectra were reported for several gaseous ions where a proton was shared between two oxygen atoms. It was suggested that in the case of an intramolecular hydrogen bond or a "proton bridge," as in the case of protonated diglyme, one would observe poor correlation between the observed IRMPD spectrum and calculated theoretical spectrum due to the anharmonicity of the double-well potential energy surface (PES) inherent to a proton bridge moiety. This point was further expanded in a study of conjugate bases of amino acids, particularly glutamate and aspartate.<sup>21</sup> Oomens et al. showed quite convincingly the effects of the anharmonicity and vibrational mode coupling due to a shared proton for the conjugate base isomers of benzenedicarboxylic acid, phthalate and terephthalate. The presence of a proton bridge resulted in spectral broadening and poor agreement between experiment and theoretical calculations. We speculate that the basicity of the carboxylate groups could result in stronger, more symmetric hydrogen bonded complexes relative to the weaker basicity of the glyme ether oxygens. At the present time we are unsure why similar broadening was not seen in this study. An alternate interpretation might be that the MP2 calculated barrier of ~6 kcal mol<sup>-1</sup> required to pass from one asymmetric structure, through the symmetrically shared proton structure, to a second asymmetric structure may be sufficiently high, when coupled with low internal energy in the ion due

## **RSCPublishing**

### ARTICLE

to "gentle" ESI formation, that the ion can remain in one configuration with a single-well potential. This would lead to more well-defined spectral peaks and better agreement with calculated harmonic vibrational frequencies.

#### **Conclusions**

Over the limited grating-tuned CO<sub>2</sub> laser output range the moderate-resolution IRMPD spectrum of protonated diglyme reported here is in quite reasonable agreement with the theoretically calculated vibrational spectrum. The experimental spectrum also validates earlier<sup>10.11</sup> results from our laboratories for which a resolved peak was seen in the 940 cm<sup>-1</sup> wavenumber range and, more generally, demonstrates that the IRMPD spectra obtained using a grating-tuned CO<sub>2</sub> laser do not show broad, unresolved spectral features, but rather defined spectral peaks.

The calculated lowest energy structure is virtually identical to one reported earlier, <sup>13</sup> obtained using the same (MP2) level of theory. Investigation of other possible structures, particularly the "tridentate" model, revealed them to be higher in energy than the reported asymmetric "bidentate" structure shown in Fig. 2.

This study allowed for comparison and further analysis of the characteristic spectral broadening of IRMPD data due to anharmonicity and vibrational mode coupling in symmetric proton-bridged ion structures. In contrast to earlier work 13,21 we did not observe spectral broadening and found good correlation between the experimentally determined IRMPD and theoretically determined vibrational spectra. It is apparent that although the IRMPD method is capable of providing detailed vibrational spectra for complex ions, certain species characterized by multiple structural conformations and extensive vibrational mode coupling require more advanced theoretical modeling to interpret the experimental data.

#### Acknowledgements

We thank Prof. Adrian Roitberg for assistance with the MP2 calculations. M. U. E. thanks the U. S. National Science Foundation under Grant OISE-0730072 for partial financial support.

#### **Notes and references**

- <sup>b</sup> Present address: Department of Physics, Kansas State University, Manhattan, KS 66506-2604, USA.
- J. Eyler, Mass Spectrom. Rev., 2009, 28, 448; N. Polfer and J. Oomens, Mass Spectrom. Rev., 2009, 28, 468; T. Fridgen, Mass Spectrom. Rev., 2009, 28, 586; N. Polfer and C. Stedwell, Lect. Notes Chem., 2013, 83, 71.
- R. Ambartzumian and V. Letokhov, Acc. Chem. Res., 1977, 10, 61; D. Lupo and M. Quack, Chem. Rev., 1987, 87, 181.
- 3 M. Stipdonk, K. Patterson, J. Gibson, G. Berden and J. Oomens, *Int. J. Mass Spectrom.*, 2015, in press. http://dx.doi.org/10.1016/j.ijms.2015.01.010.
- 4 O. Hernandez, B. Paizs and P. Maitre, *Int. J. Mass Spectrom.*, 2014, in press. http://dx.doi.org/10.1016/j.ijms.2014.08.008
- 5 M. DiTucci, S. Heiles and E. Williams, J. Am. Chem. Soc., 2015, 137, 1650.
- 6 B. Power, V. Haldys, J. Salpin and T. Fridgen, *Int. J. Mass Spectrom.*, 2014, in press. http://dx.doi.org/10.1016/j.ijms.2014.10.002
- 7 M. Butler, P. Arroyo, G. Cabrera and P. Maitre, J. Phys. Chem. A, 2014, 118, 4942.
- 8 K. Gulyuz, C. Stedwell, D. Wang and N. Polfer, *Rev. Sci. Instrum.*, 2011, **82**, 054101.
- 9 G. Baykut, C. Watson, R. Weller and J. Eyler, J. Am. Chem. Soc., 1985, 107, 8036.
- D. Peiris, M. Cheeseman, R. Ramanathan and J. Eyler, J. Phys. Chem. 1993, 97, 7839.
- 11 J. Stephenson, Jr., M. Booth, J. Shalosky, J. Eyler and R. Yost, J. Am. Soc. Mass Spectrom. 1994, 5, 886.
- 12 J. Brodbelt and J. Wilson, Mass Spectrom. Rev., 2009, 28, 390
- 13 D. Moore, J. Oomens, A. Meer, G. Helden, G. Meijer, J. Valle, A. Marshall and J. Eyler, *Chem. Phys. Chem.*, 2004, 5, 740.
- 14 M. Dole, L. Mack, R. Hines, R. Mobley, L. Ferguson and M. Alice, *J. Chem. Phys.*, 1968, **49**, 2240; J. Fenn, M. Mann, C. Meng, S. Wong and C. Whitehouse, *Science*, 1989, **246**, 64.
- 15 M. Wigger, J. Nawrocki, C. Watson, J. Eyler and S. Benner, Rapid Commun. Mass Spectrom., 1997, 11, 1749.
- 16 P. Caravatti and M. Allemann, Org. Mass Spectrom., 1991, 26, 514.
- 17 Y. Tan and N. Polfer, J. Am. Soc. Mass Spectrom., 2015, 26, 359.
- 18 S. Stefan and J. Eyler, Int. J. Mass Spectrom., 2010, 297, 96.
- 9 Gaussian 09, Revision D.01, M. Frisch, G. Trucks, H. Schlegel, G. Scuseria, M. Robb, J. Cheeseman, G. Scalmani, V. Barone, B. Mennucci, G. Petersson, H. Nakatsuji, M. Caricato, X. Li, H. Hratchian, A. Izmaylov, J. Bloino, G. Zheng, J. Sonnenberg, M. Hada, M. Ehara, K. Toyota, R. Fukuda, J. Hasegawa, M. Ishida, T. Nakajima, Y. Honda, O. Kitao, H. Nakai, T. Vreven, J. Montgomery, Jr., J. Peralta, F. Ogliaro, M. Bearpark, J. Heyd, E. Brothers, K. Kudin, V. Staroverov, T. Keith, R. Kobayashi, J. Normand, K.

<sup>&</sup>lt;sup>a</sup> Department of Chemistry, University of Florida, P.O. Box 117200, Gainesville, FL 32611-7200, USA. E-mail: eylerir@chem.ufl.edu.

PCCP RSCPublishing

## **ARTICLE**

Raghavachari, A. Rendell, J. Burant, S. Iyengar, J. Tomasi, M. Cossi, N. Rega, J. Millam, M. Klene, J. Knox, J. Cross, V. Bakken, C. Adamo, J. Jaramillo, R. Gomperts, R. Stratmann, O. Yazyev, A. Austin, R. Cammi, C. Pomelli, J. Ochterski, R. Martin, K. Morokuma, V. Zakrzewski, G. Voth, P. Salvador, J. Dannenberg, S. Dapprich, A. Daniels, O. Farkas, J. Foresman, J. Ortiz, J. Cioslowski and D. Fox, Gaussian, Inc., Wallingford CT, 2013.

- 20 http://cccbdb.nist.gov/vibscalejust.asp.
- 21 J. Oomens, J. Steill and B. Redlich, J. Am. Chem. Soc., 2009, 131, 4310.